Performance evaluation of the cognitive piggyback overlay systems with dirty paper coding

Jun Naganawa*, Kentaro Kobayashi†, Masaaki Katayama† and Takaya Yamazato‡
* Graduate School of Engineering, Nagoya University. Nagoya, Japan.
E-mail: naganawa@katayama.nuee.nagoya-u.ac.jp
† EcoTopia Science Institute, Nagoya University. Nagoya, Japan.
E-mail: {kobayasi,katayama}@nuee.nagoya-u.ac.jp
‡ Institute of Liberal Arts & Sciences, Nagoya University. Nagoya, Japan.
E-mail: yamazato@nuee.nagoya-u.ac.jp

***Abstract*—This manuscript considers a secondary system sharing the spectrum with the primary system at the same time and on the same frequency. We propose a cognitive overlay system in which the secondary system relays the primary signal and piggybacks its own data on it. Furthermore, the secondary system uses the channel coding based on the dirty paper coding (DPC). The result of the analysis shows that the proposed scheme allows the secondary system to communicate at the same speed as the primary system without any harm to it.**

I. Introduction

This paper considers spectrum sharing where two systems, primary and secondary, share the same frequency band using cognitive radio [1], [2]. In this scenario, the primary system has priority and ignores the secondary system. On the other hand, the secondary system must monitor the primary system's signal and changes its transmission and reception parameters to avoid interference to the primary system.

A typical spectrum sharing scheme using cognitive radio is "Dynamic Spectrum Access" (DSA) [3]–[5], in which the secondary system transmits its signal in the spectrum band where the primary system does not use. In other words, DSA requires that the primary system does not use all of its allocated spectrum at once and that secondary system is capable of sensing spectrum [6]–[8].

Another approach is to underlay the secondary signal using Ultra Wide Band (UWB) [9] or transmission power control (TPC) [10]–[12]. In those schemes, the secondary system sets its power spectrum density very low in order not to affect the primary system, thus the data rate of the secondary system must be slow enough to keep its power spectrum density low.

In addition to DSA and underlay schemes, Devroye et al. proposed a concept of the secondary system that cooperates with the primary system one-way [13]. They made theoretical discussion on achievable rate, but the practical model of a communication system is not proposed.

In this paper, we propose a practical cognitive overlay communication system that realizes spectrum sharing by one-sided collaboration with the primary system. In the proposed system, the secondary transmitter relays the signal of the primary system overlaid with its own data on it [14], [15]. Through the relayed primary signal acts as interference in the reception of the secondary signal, as the secondary signal is synchronized to the relayed primary signal, it is easy to apply interference cancellation at a secondary receiver [16]. In addition, taking advantage of the fact that the secondary transmitter knows the primary signal, we introduce dirty paper coding (DPC) [17], [18].

As the result of the relay operation of the primary signal, the piggybacking secondary signal does not affect the primary system. Furthermore, the proposed scheme allows the secondary system to communicate at the same speed as the primary system without any harm to it.

The outline of this paper is as follows. Section II describes the basic concept of the proposed cognitive piggyback system. Section III introduces the coding scheme based on the DPC. In Section IV, we calculate the symbol error rate at both receiver and show the numerical results in Section V. Section VI concludes this paper.

II. System model

The scenario considered in this paper is shown in Fig.1. The primary system has a pair of a transmitter and a receiver, Tx1 and Rx1, communicating using single carrier modulation scheme. The secondary system also uses a single carrier modulation using the same carrier frequency as the primary system, and has a transmitter and a receiver, Tx2 and Rx2. The impulse response of the channel between Txi and Rxj is denoted as $c_{ij}(t)$. In addition, the impulse response of the channel between Tx1 and Tx2 is denoted as $c_{10}(t)$. In this paper, for simplicity, stationary flat fading is considered, and thus the equivalent low-pass model of the response of each channel is:

$$c_{ij}(t) = H_{ij}\delta(t - \tau_{ij}), \tag{1}$$

where $|H_{ij}|$ is the propagation gain and $\arg(H_{ij})$ is the channel phase shift, while τ_{ij} is the propagation delay.

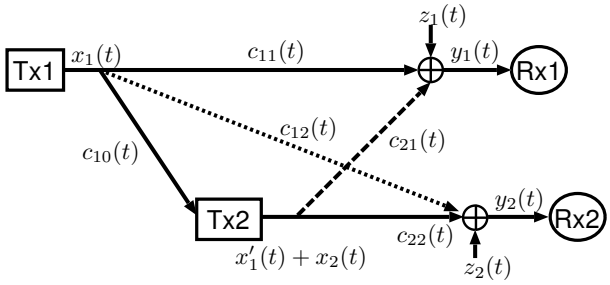

Fig. 1. System model

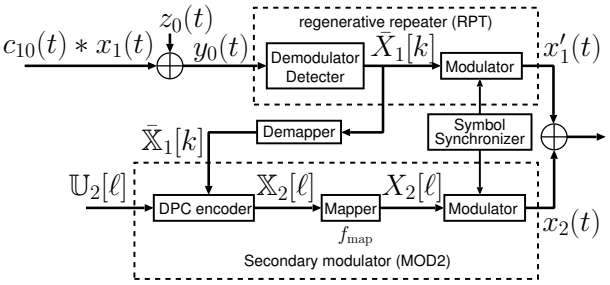

Fig. 2. Block diagram of Tx2

A. Transmitter of The Primary System: Tx1

The primary system is designed without considering the presence of the secondary system. This paper assumes that Tx1 uses conventional M-ary PSK transmitter.

The equivalent low-pass signal at the output of Tx1 is represented as

$$x_1(t) = \sqrt{P_1}\sum_k g(t-kT)X_1[k], \tag{2}$$

where T is a symbol duration, $g(t)$ is the signal pulse shape, and $X_1[k]$ is the kth symbol defined as

$$X_1[k] \in \left\{ e^{j\frac{2\pi m}{M}} \middle| m = 0,1,\ldots,M-1 \right\}. \tag{3}$$

The pulse waveform $g(t)$ is assumed to have unity energy, i.e.,

$$\int_0^T g^2(t)dt = 1, \tag{4}$$

and thus P_1 is power of $x_1(t)$.

B. Transmitter of The Secondary System: Tx2

As in Fig.1, the proposed secondary transmitter uses a signal from the primary transmitter and its own data. Fig.2 shows the block diagram of the proposed secondary transmitter Tx2. Tx2 is consist of two main blocks, i.e., the regenerative repeater (RPT) and the secondary modulator (MOD2).

In the regenerative repeater (RPT), the received signal $y_0(t)$ is first demodulated to obtain estimates of the data symbols of the primary signal expressed as

$$\bar{X}_1[k] = X_1[k]e^{j\varphi} \qquad \varphi \in \left\{ \frac{2\pi p}{M} \middle| p = 0,1,\ldots,M-1 \right\}, \tag{5}$$

where φ is the phase error in RPT. This estimates are then remodulated, and the output signal of RPT is

$$x_1'(t) = \sqrt{P_1'}\sum_k g(t-kT-\tau_{10}-\tau_\alpha)\bar{X}_1[k], \tag{6}$$

where τ_α is the processing delay in RPT.

Over the regenerated primary signal $x_1'(t)$, the secondary modulator (MOD2) transmits its own signal $x_2(t)$ of N-ary PSK modulation. For simplicity, in this paper, the secondary system uses the same symbol duration T and the same pulse shape $g(t)$ as the primary system. The pulse timing, carrier frequency and phase are synchronized with the output of RPT. Thus the output of MOD2 is

$$x_2(t) = \sqrt{P_2}\sum_l g(t-lT-\tau_{10}-\tau_\alpha)X_2[l], \tag{7}$$

where P_2 is power of $x_2(t)$, $X_2[l]$ is the lth symbol defined as

$$X_2[l] \in \left\{ e^{j\frac{2\pi n}{N}} \middle| n = 0,1,\ldots,N-1 \right\}, \tag{8}$$

which is described in Section III.

C. Receiver of The Primary System: Rx1

Since the primary system is designed without considering the presence of the secondary signal, Rx1 in Fig.1 is a conventional correlation demodulator for M-ary PSK. The input of Rx1, i.e. the sum of the signals from Tx1 and Tx2 together with AWGN $z_1(t)$, is denoted as

$$y_1(t) = c_{11}(t) * x_1(t) + c_{21}(t) * [x_1'(t) + x_2(t)] + z_1(t). \tag{9}$$

Thus Rx1 demodulates the signal and yields the decision variable for the kth symbol as follows:

$$Y_1[k] = \int_{\tau_1+kT}^{\tau_1+(k+1)T} y_1(t)g(t-kT-\tau_1)e^{-j\phi_1}dt. \tag{10}$$

In this equation, τ_1 and ϕ_1 are propagation delay and phase shift estimated in Rx1. We assume that the relayed primary signal component $c_{21}(t) * x_1'(t)$ has enough larger power than $c_{11}(t) * x_1(t)$ component, and thus Rx1 synchronizes with the signal from Tx2 [14], i.e., $\tau_1 = \tau_{10} + \tau_\alpha + \tau_{21}$ and $\phi_1 = \phi_{21}$.

D. Receiver of The Secondary System: Rx2

In contrast to the primary system, the secondary receiver is designed taking into consideration of the presence of the primary signal.

Fig.3 shows the block diagram of Rx2. The input of Rx2, i.e. the sum of the signals from Tx1 and Tx2 together with AWGN $z_2(t)$, is denoted as

$$y_2(t) = c_{12}(t) * x_1(t) + c_{22}(t) * [x_1'(t) + x_2(t)] + z_2(t). \tag{11}$$

Rx2 first demodulates the primary signal as Rx1 does, which yields the decision variable for the kth symbol as follows:

$$Y_2[k] = \int_{\tau_2+kT}^{\tau_2+(k+1)T} y_2(t)g(t-kT-\tau_2)e^{-j\phi_2}dt, \tag{12}$$

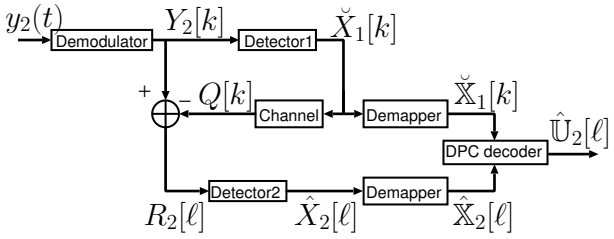

Fig. 3. Block diagram of Rx2

where τ_2 and ϕ_2 are propagation delay and phase shift corresponding to the kth symbol of the primary system. As in the case of Rx1, Rx2 also synchronizes to the signal from Tx2. Thus $\tau_2 = \tau_{10} + \tau_\alpha + \tau_{22}$ and $\phi_2 = \phi_{22}$.

Based on the decision variable $Y_2[k]$, Detector1 recovers the transmitted symbol of the primary system as $\breve{X}_1[k]$. Next, $\breve{X}_1[k]$ is multiplied by channel response $c_{22}(t)$ to yield $Q[k]$, which is the estimate of the primary signal component from Tx2. Subtracting $Q[k]$ from $Y_2[k]$, we have

$$R_2[l] = Y_2[k] - Q[k], \tag{13}$$

which is the sum of the secondary signal component, the residual primary signal component from Tx1 and noise component. Detector2 uses this decision variable to find the estimate of the secondary symbol $\hat{X}_2[l]$, further process are described in the following sections.

III. Proposed Coding Scheme Based on the Dirty Paper Coding

In the reception of the secondary signal at Rx2, dominant cause of interference is the primary signal relayed by Tx2. In this scenario, since Tx2 knows both the information of the secondary signal and the interfering primary signal, dirty paper coding (DPC) [17], [18] can be introduced in the secondary system.

On the transmitting side, Tx2, let us define $\mathbb{U}_2[l]$ in Fig.2 as the information bit sequences of length $\log_2 N$ corresponding to the lth symbol. In a similar way, let $\bar{\mathbb{X}}_1[k]$ be the bit sequence with the length of $\log_2 M$ corresponding to the regenerated kth primary symbol. For simplicity, this paper assumes that both the primary and the secondary systems use the same modulation index ($M = N$), then the dirty paper encoder output is:

$$\mathbb{X}_2[l] = \mathbb{U}_2[l] \oplus \bar{\mathbb{X}}_1[k], \tag{14}$$

where $\oplus$ denotes bit-by-bit modulo-two addition and $\mathbb{X}_2[l]$ is the bit sequences transmitted by the N-ary PSK symbol, $X_2[l]$. We assume that the mapping function from $\mathbb{X}_2[l]$ to $X_2[l]$ is defined as f_{map} with gray coding.

On the receiving side, Rx2 in Fig.3, a bit sequence corresponding to $\bar{\mathbb{X}}_1[k]$, i.e., $\breve{\mathbb{X}}_1[k]$, is generated from the output of Detector1. At the same time, an estimate of $\mathbb{X}_2[l]$, $\hat{\mathbb{X}}_2[l]$, is generated from $\hat{X}_2[l]$. Using these two bit sequences, $\breve{\mathbb{X}}_1[k]$ and $\hat{\mathbb{X}}_2[l]$, we can decode the transmitted information bits $\mathbb{U}_2[l]$ as

$$\hat{\mathbb{U}}_2[l] = \breve{\mathbb{X}}_1[k] \oplus \hat{\mathbb{X}}_2[k]. \tag{15}$$

IV. Symbol Error Rate and Channel Capacity

In this section, the symbol error rates of Rx1 and Rx2 are analytically derived. In the rest of this paper, for ease of discussion, propagation delays τ_{ij} are ignored and the delay in RPT τ_α is assumed to be an integral multiple of T.

A. Symbol Error Rate at Rx1

From (2), (6), (7), (9), and (10), the decision variable $Y_1[k]$ is expressed as

$$\begin{aligned} Y_1[k] &= \sqrt{P_1} H_{11} X_1[k+n_0] e^{-j\phi_{21}} \\ &\quad + \sqrt{P_1'} |H_{21}| \bar{X}_1[k] + \sqrt{P_2} |H_{21}| X_2[l] + Z_1[k] \\ &= \Upsilon_1[k] + Z_1[k], \end{aligned} \tag{16}$$

where $n_0 = \tau_\alpha / T > 0$ and $\Upsilon_1[k]$ is the sum of terms corresponding information symbols. As $z_1(t)$ is AWGN, $Z_1[k]$ is an independent zero-mean complex Gaussian random variable with the variance σ_1^2. Since only $Z_1[k]$ is a random variable in (16), $Y_1[k]$ is a complex Gaussian random variable with probability density function

$$p_1(Y_1[k]) = \frac{1}{2\pi\sigma_1^2} \exp\left[-\frac{|Y_1[k] - \Upsilon_1[k]|^2}{2\sigma_1^2} \right]. \tag{17}$$

With this distribution of $Y_1[k]$, the probability that $\hat{X}_1[k] = X_m$, is:

$$\Pr(\hat{X}_1[k] = X_m) = \int_{D_{1,m}} p_1(Y_1[k]) dY_1[k], \tag{18}$$

$$D_{1,m} = \left\{ |\arg(Y_1[k]) - \arg(X_m)| < \frac{\pi}{M} \right\}, \tag{19}$$

where $X_m = \exp(j\frac{2\pi}{M} m)$, for $m = 0, 1, \ldots, M-1$. With this probability, the symbol error rate P_{M1} is described as

$$P_{M1} = 1 - \mathbf{E}\left[\Pr\left(\hat{X}_1[k] = X_1[k] \right) \right], \tag{20}$$

where $\mathbf{E}[\cdot]$ is ensemble average for all possible values of $\bar{X}_1[k]$, $X_2[l]$, and $X_1[k+n_0]$.

B. Symbol Error Rate at Rx2

From (2), (6), (7), (11), and (12), the decision variable $Y_2[k]$ at the output of the demodulator of Rx2 in Fig.3 is

$$\begin{aligned} Y_2[k] &= \sqrt{P_1} H_{12} X_1[k+n_0] e^{-j\phi_{22}} \\ &\quad + \sqrt{P_1'} |H_{22}| \bar{X}_1[k] + \sqrt{P_2} |H_{22}| X_2[l] + Z_2[k] \\ &= \Upsilon_2[k] + Z_2[k], \end{aligned} \tag{21}$$

where $\Upsilon_2[k]$ is the sum of terms corresponding to information symbols. Let us define the variance of $Z_2[k]$ as σ_2^2. Then $Y_2[k]$ is a complex Gaussian random variable with probability density function

$$p_1'(Y_2[k]) = \frac{1}{2\pi\sigma_2^2} \exp\left[-\frac{|Y_2[k] - \Upsilon_2[k]|^2}{2\sigma_2^2} \right]. \tag{22}$$

With this distribution, the probability that the decision of Detector1 becomes X_m is:

$$P(\breve{X}_1[k] = X_m) = \int_{D_{1,m}'} p_1'(Y_2[k]) dY_2[k], \tag{23}$$

$$D_{1,m}' = \left\{ |\arg(Y_2[k]) - \arg(X_m)| < \frac{\pi}{M} \right\}. \tag{24}$$

After estimating $\breve{X}_1[k]$, Rx2 regenerates the primary signal component in $Y_2[k]$, for interference cancellation:

$$Q[k] = \sqrt{P_1'}|H_{22}|\breve{X}_1[k]. \quad (25)$$

The result of the cancellation is thus

$$\begin{aligned} R_2[l] &= Y_2[k] - Q[k] \\ &= \Upsilon_2[k] - Q[k] + Z_2[k]. \end{aligned} \quad (26)$$

Note that $R_2[l]$ is a complex Gaussian random variable with mean $\Upsilon_2[k] - Q[k]$ and variance σ_2^2; its probability density function is

$$p_2(R_2[l]) = \frac{1}{2\pi\sigma_2^2} \exp\left[-\frac{|R_2[l] - \Upsilon_2[k] - Q[k]|^2}{2\sigma_2^2}\right]. \quad (27)$$

Thus the probability of correct detection of $\hat{X}_2[l]$ after interference cancellation with $Q[k]$ is

$$P\left(\hat{X}_2[l] = X_n \middle| \breve{X}_1[k] = X_m\right) = \int_{D_{2,n}} p_2(R_2[l]) dR_2[l], \quad (28)$$

$$D_{2,n} = \left\{ |\arg(R_2[l]) - \arg(X_n)| < \frac{\pi}{M} \right\}. \quad (29)$$

The symbol error rate without coding P_{M2}(w/o DPC) is then

$$P_{M2}(\text{w/o DPC}) = 1 - \mathbf{E}\left[\Pr\left(\hat{X}_2[l] = X_2[l] \middle| \breve{X}_1[k]\right)\right], \quad (30)$$

where $\mathbf{E}[\cdot]$ is ensemble average for all possible equal probable $X_1[k+n_0]$, $\breve{X}_1[k]$ of (23), and $X_2[l]$.

On the other hand, the symbol error rate with dirty paper coding becomes as follows:

$$\begin{aligned} P_{M2}(\text{w/ DPC}) &= \Pr(\hat{\mathbb{U}}_2[l] \neq \mathbb{U}_2[l]]) \\ &= \Pr(\hat{\mathbb{X}}_2[l] \oplus \breve{\mathbb{X}}_1[k] \neq \mathbb{U}_2[l]) \\ &= \Pr(\hat{\mathbb{X}}_2[l] \neq \mathbb{U}_2[l] \oplus \breve{\mathbb{X}}_1[k]) \\ &= 1 - \mathbf{E}\left[\Pr\left(\hat{X}_2[l] = X_2'[l] \middle| \breve{X}_1[k]\right)\right], \end{aligned} \quad (31)$$

where $X_2'[l] = f_{\text{map}}\left(\mathbb{U}_2[l] \oplus \breve{\mathbb{X}}_1[k]\right)$, $\mathbf{E}[\cdot]$ is ensemble average not only for $X_1[k+n_0]$, $\breve{X}_1[k]$ but also $\bar{X}_1[k]$ and $\mathbb{U}_2[l]$.

C. Channel capacity of the secondary system

The transmission of a M-ary symbol of the secondary system from Tx2 to Rx2 can be regarded as a $M \times M$ discrete memoryless channel (DMC). The conditional probability of the channel output is conditioned by its input defined as

$$\begin{aligned} P(\hat{\mathbb{U}}_2[l] | \mathbb{U}_2[l]) &= \mathbf{E}\left[\Pr\left(\hat{\mathbb{X}}_2[l] \middle| \mathbb{X}_2[l]\right)\right] \\ &= \mathbf{E}\left[\Pr\left(\hat{X}_2[l] \middle| \breve{X}_1[k]\right)\right], \end{aligned} \quad (32)$$

where $\mathbf{E}[\cdot]$ is ensemble average for possible values of $\breve{\mathbb{X}}_1[k]$, $\bar{\mathbb{X}}_1[k]$ and $X_1[k+n_0]$. Then the channel capacity is defined as [19]

$$C_2 = \frac{1}{M} \sum_{\mathbb{U}_2[l]} \sum_{\hat{\mathbb{U}}_2[l]} P(\hat{\mathbb{U}}_2[l] | \mathbb{U}_2[l]) \log_2 \left[M P(\hat{\mathbb{U}}_2[l] | \mathbb{U}_2[l]) \right]. \quad (33)$$

V. NUMERICAL RESULTS

This section shows the performance of the proposed scheme using QPSK or 8PSK modulation for both the primary and the secondary systems ($M = N = 4$ or 8). The channel gains $|H_{ij}|$ are set so that $|H_{11}| = |H_{12}| = |H_{10}|$ and $|H_{21}| = |H_{22}|$. The values that the symbol error rate of each receiver becomes worst are used for the channel phase shifts ϕ_{21} and ϕ_{22}. Furthermore, the power ratio of relayed and direct components of the primary signal at each receiver is defined as

$$\gamma_h = 10 \log \frac{|H_{21}|^2 P_1'}{|H_{11}|^2 P_1} = 10 \log \frac{|H_{22}|^2 P_1'}{|H_{12}|^2 P_1}. \quad (34)$$

In addition, the power ratio of the secondary signal and the relayed primary signal at Tx2 is defined as

$$\lambda = 10 \log \frac{P_2}{P_1'}. \quad (35)$$

A. Symbol error rate of the primary system

Fig.4 shows the symbol error rate (SER) at Rx1, where $\gamma_h = 20$[dB] and $\lambda = -10$[dB]. This figure shows that the performance of the primary system is not degraded by the presence of the secondary system. The signal bearing data of the secondary system, $x_2(t)$, may degrade the performance of Rx1, but at the same time the improvement in signal to noise ratio by relayed primary signal $x_1'(t)$ helps the primary signal reception at Rx1. As the result, performance of Rx1 remains the same.

Fig.5 shows the influence of the power of the secondary signal on the SER performance of the primary signal. The SER performance of the primary system without the secondary signal are also show in the figure using triangles. This figure confirms that the secondary signal does not degrade the performance of the primary system much , if λ is kept below a certain threshold. From this viewpoint, the maximum allowed signal power ratio of the secondary system is $\lambda = -2$[dB] ($P_2 = 0.63P_1' = 63P_1$) in the case of QPSK, and $\lambda = -8$[dB] ($P_2 = 0.16P_1' = 16P_1$) in the case of 8PSK.

The upper bound of the maximum allowable value of λ can be derived as follows. Assume that the interference from the secondary signal dominate the performance at Rx and that the noise component of (16) is ignored, then the decision error at Rx1 does not occur if

$$|\arg(\Upsilon_1[k]) - \arg(X_1[k])| \leq \frac{\pi}{M}. \quad (36)$$

Thus the upper bound of the maximum allowed signal power ratio of the secondary system can be defined as

$$\lambda_{\max} = \underset{\lambda}{\text{argmax}} \max_{\substack{X_1[k+n_0], \\ X_2[l], \phi_{21}}} \left\{ \left| \arg(\Upsilon_1[k]) - \arg(\bar{X}_1[k]) \right| = \frac{\pi}{M} \right\}, \quad (37)$$

which can be rewrite as

$$\lambda_{\max} = 20 \log \left[\frac{\sin\left(\frac{\pi}{M}\right)}{\sin(\frac{\pi}{2} - \frac{\pi}{M})} \right]. \quad (38)$$

This equation provides tight upper bounds, i.e., $\lambda_{\max} \leq 0$[dB] in the case of QPSK, $\lambda_{\max} \leq -7.7$[dB] in the case of 8PSK.

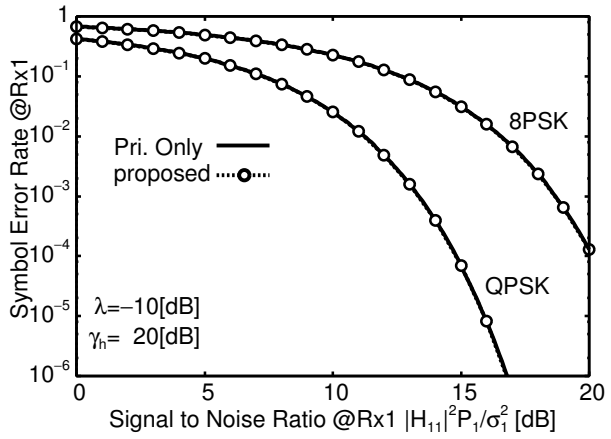

Fig. 4. The symbol error rate at Rx1 with QPSK and 8PSK

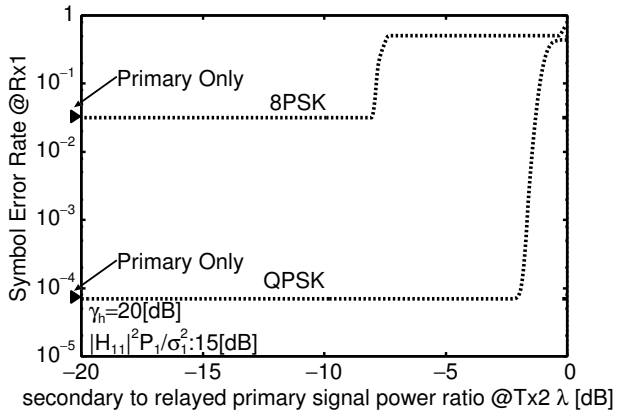

Fig. 5. The symbol error rate at Rx1 based on the secondary power with QPSK and 8PSK

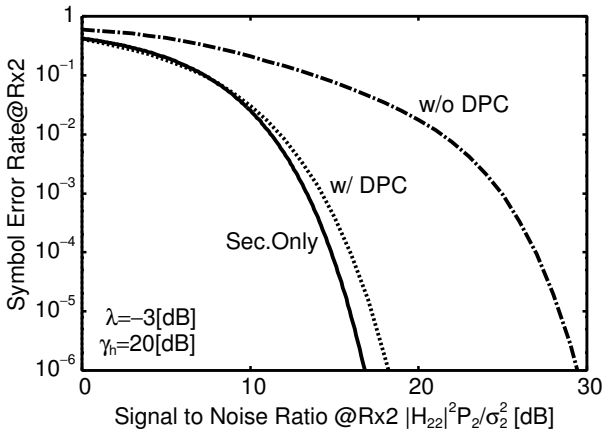

Fig. 6. The symbol error rate at Rx2 with QPSK

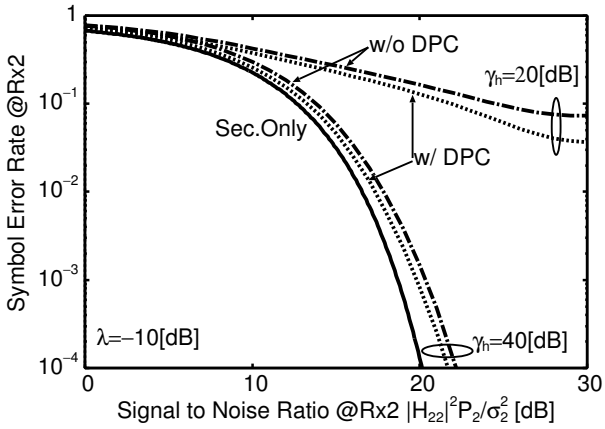

Fig. 7. The symbol error rate at Rx2 with 8PSK

B. Symbol Error Rate and channel capacity of the secondary system

In Figs.4 and 5, we have confirmed that there is a region of λ, in which the primary system is not degraded by the presence of the secondary signal. The next question is the performance of the secondary system under the same condition.

Fig.6 shows the SER performance of the secondary system with/without DPC using QPSK where $\lambda = -3$[dB]. Note that Fig.5 ensures no degradation in the performance of the primary system with the parameters chosen for Fig.6. In Fig.6, the SER of the secondary system under the presence of the primary signal is worse than that without the primary signal, but the degradation is less than 2[dB] with DPC. Hence, if the secondary system accepts this degradation, it can communicate using the same spectrum of the primary system without harming it. Note that the degradation is more than 11[dB] without DPC. Thus, the coding gain of proposed scheme is 9[dB] in this case.

Fig.7 shows the SER performance of the secondary system with/without DPC using 8PSK where $\gamma_h = 20, 40$[dB] and $\lambda = -10$[dB]. In contrast with the QPSK, when $\gamma_h = 20$[dB] as in Figs.4-6, the presence of the primary signal largely degrade the SER performance of the secondary system. This is because of the higher sensitivity for interference of 8PSK than QPSK. However, when the output power of Tx2 is larger, $\gamma_h = 40$[dB] in Fig.7, the interference from Tx1 is decreased, and thus with little influence to the primary system the secondary system can communicate at the same spectrum of the primary (system) with less than 2[dB] penalty.

Fig.8 shows the channel capacity of the secondary system with/without DPC using QPSK and 8PSK where $\gamma_h = 20$[dB], $\lambda = -3$[dB] in the case of QPSK and $\gamma_h = 40$[dB], $\lambda = -10$[dB] in the case of 8PSK. This figure shows that the capacity of the secondary system remains high even when the primary signal exists,especially if DPC is employed.

VI. Conclusions

In this paper, we propose a cognitive radio secondary system based on one-way collaboration with the primary system. This secondary transmitter relays the primary signal and piggybacks its own data on it. In addition, the secondary system uses the coding scheme based on the dirty paper coding.

As the result, it is found that the proposed secondary system can communicate on the same frequency of the primary system at high data rate without harm to the primary system if the secondary system selects adequate own symbol power.

The introduction of DPC improves SER performance without changing data rate, and thus provides higher capacity for the secondary system, especially for QPSK modulation.

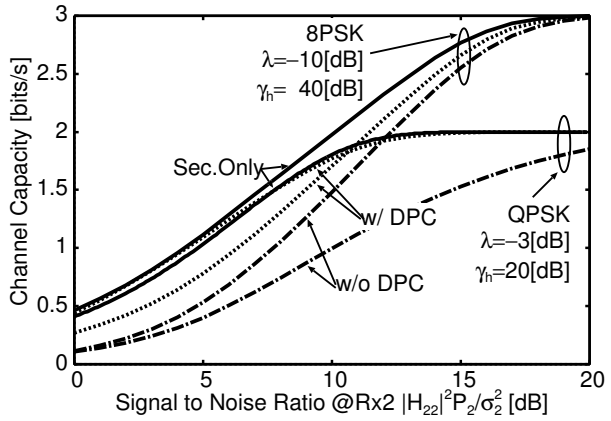

Fig. 8. The channel capacity of the secondary system with QPSK and 8PSK

The conclusions given in this paper are drawn under AWGN conditions. The consideration of multi-path fading environments is one of future topics. In addition, as a future work, we will apply the quadrature amplitude modulation and orthogonal frequency division multiplexing into the proposed scheme.

REFERENCES

[1] J. Mitola III and G. Q. Maguire Jr., "Cognitive radio: making software radios more personal," *IEEE Personal Communications*, vol. 6, no. 4, pp. 13–18, Aug. 1999.

[2] S. Haykin, "Cognitive radio: brain-empowered wireless communications," *IEEE J. Sel. Areas Commun.*, vol. 23, no. 2, pp. 201–220, Feb. 2005.

[3] Q. Zhao and B. M. Sadler, "A survey of dynamic spectrum access," *IEEE Signal Process. Mag.*, vol. 24, no. 3, pp. 79–89, May 2007.

[4] S. A. Jafar and S. Srinivasa, "Capacity limits of cognitive radio with distributed and dynamic spectral activity," *IEEE J. Sel. Areas Commun.*, vol. 25, no. 3, pp. 529–537, Apr. 2007.

[5] C. Stevenson, G. Chouinard, Z. Lei, W. Hu, S. Shellhammer, and W. Caldwell, "IEEE 802.22: The first cognitive radio wireless regional area network standard," *IEEE Commun. Mag.*, vol. 47, no. 1, pp. 130–138, Jan. 2009.

[6] G. Ganesan and Y. G. Li, "Cooperative spectrum sensing in cognitive radio, part i: Two user networks," *IEEE Trans. Wireless Commun.*, vol. 6, no. 6, pp. 2204–2213, Jun. 2007.

[7] R. Chen, J.-M. Park, Y. T. Hou, and J. H. Reed, "Toward secure distributed spectrum sensing in cognitive radio networks," *IEEE Commun. Mag.*, vol. 46, no. 4, pp. 50–55, Apr. 2008.

[8] A. Ghasemi and E. S. Sousa, "Spectrum sensing in cognitive radio networks: requirements, challenges and design trade-offs," *IEEE Commun. Mag.*, vol. 46, no. 4, pp. 32–39, Apr. 2008.

[9] H. Zhang, X. Zhou, K. Y. Yazdandoost, and I. Chlamtac, "Multiple signal waveforms adaptation in cognitive ultra-wideband radio evolution," *IEEE J. Sel. Areas Commun.*, vol. 24, no. 4, pp. 878–884, Apr. 2006.

[10] Y. Chen, G. Yu, Z. Zhang, H. hwa Chen, and P. Qiu, "On cognitive radio networks with opportunistic power control strategies in fading channels," *IEEE Trans. Wireless Commun.*, vol. 7, no. 7, pp. 2752–2761, Jul. 2008.

[11] H. Islam, Y. chang Liang, and A. Hoang, "Joint power control and beamforming for cognitive radio networks," *IEEE Trans. Wireless Commun.*, vol. 7, no. 7, pp. 2415–2419, Jul. 2008.

[12] B. Mark and A. Nasif, "Estimation of maximum interference-free power level for opportunistic spectrum access," *IEEE Trans. Wireless Commun.*, vol. 8, no. 5, pp. 2505–2513, May 2009.

[13] N. Devroye, P. Mitran, and V. Tarokh, "Achievable rates in cognitive radio channels," *IEEE Trans. Inf. Theory*, vol. 52, no. 5, pp. 1813–1827, May 2006.

[14] J. Naganawa, T. Yamazato, and M. Katayama, "Cognitive radio with relay of a primary signal and piggyback modulation," *IEEE International Symposium on Personal, Indoor and Mobile Radio Communication*, Sep. 2009.

[15] ——, "An application of regenerative relay to the cognitive piggyback overlay system (in japanese)," *IEICE Technical Report*, vol. 109, no. 383, pp. 9–14, Jan. 2010.

[16] ——, "Introduction of dirty paper coding for the cognitive piggyback overlay systems (in japanese)," *IEICE General conference*, vol. B-17-9, p. 652, Mar. 2010.

[17] M. H. M. Costa, "Writing on dirty paper," *IEEE Trans. Inf. Theory*, vol. 29, no. 3, pp. 439–441, May 1983.

[18] A. Khisti, U. Erez, A. Lapidoth, and G. W. Wornell, "Carbon copying onto dirty paper," *IEEE Trans. Inf. Theory*, vol. 53, no. 5, pp. 1814–1827, May 2007.

[19] J. G. Proakis, *Digital Communications*, 4th ed. McGraw-Hill, 2001.